Semi-Empirical Nonlinear Site Amplification from NGA-West2 Data and Simulations

Emel Seyhan[a] M.EERI, **and Jonathan P. Stewart**[b] M.EERI

We analyze NGA-West2 data and simulations to develop a site amplification model that captures ground motion scaling with V_{S30} and soil nonlinear effects. We parameterize nonlinearity as the gradient of site amplification with respect to peak acceleration for reference (firm) sites. Both data analyses and simulations indicate nonlinearity for sites with $V_{S30} < 500$ m/s and spectral periods $T < \sim 3$ s. Following approximate removal of nonlinear effects from the data, we evaluate V_{S30}-scaling of ground motions, which is most pronounced for $T \geq \sim 0.2$ s and saturates for hard rock sites. Regional trends in V_{S30}-scaling and nonlinearity were not found to be sufficiently robust to justify inclusion in our model. We apply the site amplification model to derive site factors now approved for building code applications. Principal causes of changes relative to previous values are reduction of the reference velocity (at which amplification is unity) to 760 m/s and reduced nonlinearity. [DOI: 10.1193/063013EQS181M]

INTRODUCTION

Site factor terms in the NGA-West2 (and many earlier) ground motion prediction equations (GMPEs) express the effect of shallow site conditions on various ground motion intensity measures (IMs) as a function of V_{S30}. The parameter V_{S30} represents the average shear wave velocity of a site in the upper 30 m, and is computed as the ratio of 30 m to shear wave travel time through the upper 30 m of the site. Site factors in the NEHRP *Provisions*, which are used in building codes worldwide and also in financial loss modeling for insurance applications, are based on site categories derived from V_{S30}. Seyhan and Stewart (2012) describe substantial differences between site factors from the original NGA GMPEs and those in the NEHRP *Provisions*, which is problematic in engineering practice.

In this paper, we describe the development of a semi-empirical site amplification model derived from NGA-West2 data analysis and our interpretation of one-dimensional (1-D) ground response simulation results by Kamai et al. (2014). The resulting model is adopted as the site term in the Boore et al. (2014) GMPE and is used to derive site factors now approved for the 2015 NEHRP *Provisions*.

[a] Risk Management Solutions, Newark, CA (formerly UCLA Civil & Environmental Engineering Department)
[b] University of California, Los Angeles, Civil & Environmental Engineering Dept., Los Angeles, CA, 90095

Earthquake Spectra, Volume 30, No. 3, pages 1241–1256, August 2014;

EQUATIONS FOR NONLINEAR SITE AMPLIFICATION MODEL

The site amplification model comprises two additive terms representing V_{S30}-scaling and nonlinearity as follows:

$$F_{S,B} = \ln(F_{lin}) + \ln(F_{nl}) \tag{1}$$

where $F_{S,B}$ represents "base case" (ignoring basin effects) site amplification in natural logarithmic units; F_{lin} represents the linear component of site amplification, which is dependent on V_{S30}; and F_{nl} represents the nonlinear component of site amplification, which depends on V_{S30} and the amplitude of shaking on reference rock (taken as $V_{S30} = 760$ m/s).

The linear component of the model (F_{lin}) describes the scaling of ground motion with V_{S30} for linear soil response conditions (i.e., small strains) as follows:

$$\ln(F_{lin}) = \begin{cases} c \ln\left(\frac{V_{S30}}{V_{ref}}\right) & V_{S30} \leq V_c \\ c \ln\left(\frac{V_c}{V_{ref}}\right) & V_{S30} > V_c \end{cases} \tag{2}$$

where c describes the V_{S30}-scaling in the model, V_c is the limiting velocity beyond which ground motions no longer scale with V_{S30}, and V_{ref} is the site condition for which the amplification is unity (taken as 760 m/s).

The nonlinear term in the site amplification model (F_{nl}) modifies the linear site amplification in order to decrease amplification for strong shaking levels. The F_{nl} term is constructed to produce no change relative to the linear term for low PGA_r levels. The functional form for F_{nl} is as follows:

$$\ln(F_{nl}) = f_1 + f_2 \ln\left(\frac{PGA_r + f_3}{f_3}\right) \tag{3}$$

where f_1, f_2, and f_3 are coefficients in the model, and PGA_r is the median peak horizontal acceleration for reference rock (taken as $V_{S30} = 760$ m/s). We take $f_1 = 0$ to force $\ln(F_{nl})$ to 0 for $PGA_r \ll f_3$. Parameter f_3 is set as 0.1 g. Parameter f_2 is a function of period and V_{S30} as follows:

$$f_2 = f_4[\exp\{f_5(\min(V_{S30}, 760) - 360)\} - \exp\{f_5(760 - 360)\}] \tag{4}$$

where f_4 and f_5 are period-dependent coefficients. This functional form for f_2 is the same as that used by Chiou and Youngs (2008). Model coefficients and a coded version of the model in Matlab are given as part of the online Appendix to this paper.

MODEL DEVELOPMENT

The model was developed in two stages, the first to develop the nonlinear model and the second to develop the V_{S30}-scaling model. The sections below describe the data utilized, the two stages of model development, and issues related to regional variations of site response.

GROUND MOTION DATABASE

We utilize the ground motion database described in Ancheta et al. (2014) along with the site database for ground motion recording stations by Seyhan et al. (2014). The data-selection criteria match those of the Phase 3 analysis of Boore et al. (2014). We defer to that publication for details, but some of the major elements of the selection criteria unique to this work include the use of Class 1 and 2 events (commonly known as main shocks and aftershocks, respectively), and a magnitude (**M**) and distance cutoff intended to remove bias from poor sampling of distant stations (e.g., only recordings under 400 km distance are used for $\mathbf{M} > 6$ earthquakes recorded by modern digital instruments). As discussed further below, problems with regional variations in anelastic attenuation effects that arise from the use of data at large site-source distances are accounted for in the analysis of site factors.

STAGE 1 ANALYSIS OF NONLINEAR SITE RESPONSE

The Stage 1 analyses develop estimates of parameter f_2 (defined in Equation 3) on the basis of available simulations and from the interpretation of NGA-West2 data. The considered simulations are of one-dimensional (1-D) equivalent-linear ground response for many site profiles and input motions (Kamai et al. 2014; hereafter, KEA14).

The NGA-West2 data analysis begins with the computation of rock residuals for each recording in the selected data set:

$$R_{ij} = \ln Y_{ij} - [(\mu_r)_{ij} + \eta_i] \tag{5}$$

where R_{ij} is the within-event rock residual, Y_{ij} is the j^{th} observed (recorded) value of the ground-motion IM, μ_r is the mean (in natural log units) of a GMPE for rock conditions, and η_i is the event term for earthquake i. We use the rock site condition of $V_{S30} = 760$ m/s. Regarding the GMPE used to compute μ_r, our analyses were performed iteratively with respect to the development of the Boore et al. (2014) GMPEs (hereafter, BEA14). Essentially, we began with an early version of the Campbell and Bozorgnia (2014) GMPEs, from which a preliminary site amplification model was developed. That site model was then used in a subsequent derivation of preliminary source and path terms in the BEA14 GMPEs. There were many subsequent iterations in this process, but the critical point to be made is that the site terms presented here are fully compatible with the base-case GMPEs presented by BEA14. Those GMPEs include adjustments for regional apparent anelastic attenuation effects, which substantially affect the amount of data considered in analyses for site effects (details in a subsequent section titled *Regional Effects*).

To investigate nonlinearity, we compile values of R_{ij} within bins of V_{S30} ($\leq$200, 200–310, 310–520, 520–760, $\geq$760 m/s), which are plotted against PGA_r in Figure 1. We use least-squares regression to fit to the data an expression of the form given in Equation 3 with f_3 fixed at 0.1 g (justification given in Section A.2 of the online Appendix) to provide estimates of f_1 and f_2. Nonlinearity is manifest in the plots by non-zero values of slope parameter f_2 that are statistically significant, which is judged to be the case when the value of f_2 is larger than its standard error (marked with a star in Figure 1). There are two major trends in the plots, both of which have been observed previously (e.g., Choi and Stewart 2005):

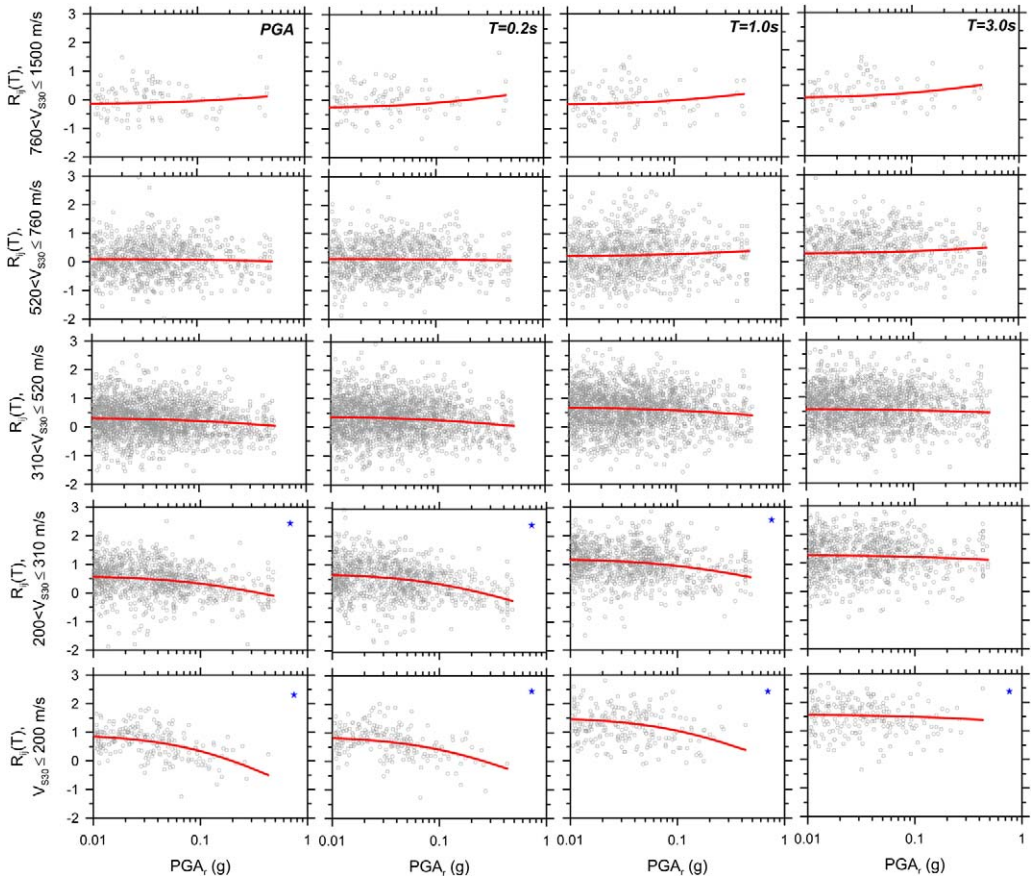

Figure 1. Variation of site amplification factors with PGA_r within V_{S30} bins using full data set. Discrete symbols are intra-event residuals (R_{ij}, Equation 5); line is nonlinear fit from Equation 4. The star symbol indicates that the slope parameter fit to the data is significantly different from zero.

(1) nonlinearity decreases with increasing V_{S30}, generally becoming statistically insignificant for relatively stiff sites; and (2) nonlinearity decreases as period increases, being statistically significant only for $T \leq \sim 1$ s, except for the softest soil sites ($V_{S30} < 200$ m/s).

The nonlinear component of the site amplification models can also be derived on the basis of equivalent-linear 1-D ground response simulations in lieu of empirical data analysis (this approach is used in the NGA-West2 GMPEs by Abrahamson et al. 2014 and Campbell and Bozorgnia 2014). The original NGA project utilized simulations described by Walling et al. (2008; hereafter, WEA08). In NGA-West2, KEA14 analyzed a larger simulation set with additional site profiles and input motions. The nonlinearity in simulation-based site amplification is driven by the shear modulus reduction and damping (MRD) versus shear strain relations used in the calculations. Both WEA08 and KEA14 used judgment-driven MRD curves known as the peninsular range curves (PEN) and curves presented by

EPRI (1993). The simulation results are presented as period-dependent nonlinear amplification equations for discrete V_{S30} values. The equations are structured similarly to Equation 3 but are considerably more complex such that the coefficients' physical meaning is not the same as f_1, f_2, and f_3. Accordingly, as described further in Section A.1 of the online Appendix, we fit Equation 3 to KEA14 model predictions to obtain f_2, values, which are shown in Table 1 (additional coefficients f_1 and f_3 were also obtained but are of less interest). Results in Table 1 are given for the discrete V_{S30} values for which amplification models are available from KEA14.

Figure 2 shows values of the nonlinear parameter f_2 from data analysis and simulations. Also shown are slopes evaluated by Afacan et al. (2014; hereafter, AEA14), using a fitting procedure similar to that described above, based on centrifuge modeling of soft clays. The simulation-based slopes are comparable to the data-based slopes, except for 5% damped pseudo-spectral accelerations (PSAs) at $T = 0.5{-}3.0$ s, where the data exhibit more nonlinearity than is evident from the simulations. These variations in slopes may reflect differences between the average soil properties (V_S profiles and nonlinear relationships) at the NGA-West2 sites and those used in simulations, or could result from limitations of the 1-D equivalent-linear analysis method.

The slopes derived from centrifuge modeling (at $V_{S30} = 100{-}125$ m/s) are generally similar to those at the lower limit of V_{S30} (~150–200 m/s) from simulations and data analysis, with the exception of PGA and positive values of slope for $T > 1$ s. These results suggests that a minimum floor on nonlinearity may be present for very soft sites, although such a feature is not presently included in our model, which we consider applicable for V_{S30} as low as 150 m/s. We elected to not allow the model to produce positive values of f_2.

The nonlinear term f_2 is parameterized relative to V_{S30} following the function of Chiou and Youngs (2008), as given in Equation 4. Parameter f_4 controls the overall level of nonlinearity for soft soils and was adjusted to produce a good visual fit to the data and simulation results, as shown by the model curves in Figure 2. Where the slopes from simulations and

Table 1. Values of f_2 for KEA14 model based on fit using Equation 3

	PEN MRD Model (V_{S30} values in m/s)					
Period (s)	190	270	400	560	760	900
0.01	−0.48	−0.34	−0.17	−0.05	0.00	0.00
0.2	−0.77	−0.52	−0.23	−0.03	0.00	0.00
1	−0.38	−0.13	0.00	0.00	0.00	0.00
3	0.14	0.05	0.00	0.00	0.00	0.00
	EPRI MRD Model (V_{S30} values in m/s)					
Period (s)	–	270	400	560	760	–
0.01	–	−0.36	−0.27	−0.17	−0.09	–
0.2	–	−0.60	−0.39	−0.23	−0.10	–
1	–	0.02	0.00	0.00	0.00	–
3	–	0.16	0.09	0.03	0.00	–

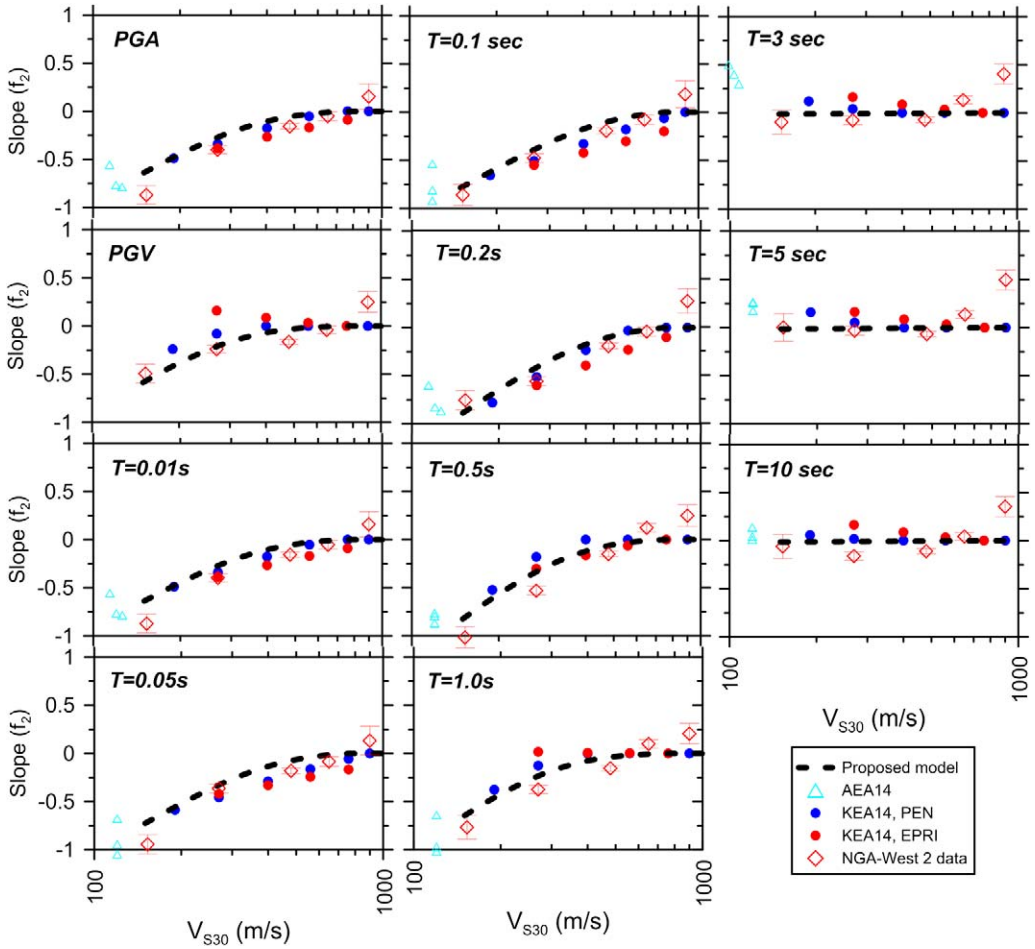

Figure 2. Variation of slope f_2 with V_{S30} from NGA-West2 data including 95% confidence intervals, KEA14 simulations (using modulus reduction curves labeled PEN for Peninsular range and EPRI), centrifuge modelling (Afacan et al. 2014; AEA14), and proposed model.

data diverge (e.g., PSA at $T = 0.5 - 3.0$ s), more weight is given to slopes derived from data. Parameter f_5 controls the shape of the V_{S30} dependency of the slope f_2; no adjustments relative to the values given by Chiou and Youngs (2008) were found to be needed, so those values were adopted.

STAGE 2 ANALYSIS OF V_{S30} SCALING

We begin with residuals R_{ij} (Equation 5), which are adjusted by removing nonlinear effects as predicted by the F_{nl} model (Equation 3):

$$R_k^{lin} = R_{ij} - \ln(F_{nl})_{ij} \tag{6}$$

The modified residual, R_k^{lin}, is intended to apply for linear (small-strain) conditions. Subscript k in R_k^{lin} is an index spanning across all available data points; we drop the event and within-event subscripts (i and j, respectively) because of the removal of event terms in the computation of R_{ij}, which allows all data points to be weighted equally. The residuals for the full (combined) data set and individual regions are then regressed in a least-squares sense against V_{S30} (using Equation 2) to establish the c parameter for $V_{S30} < V_c$. Results for several periods and the combined (non-regionalized) data set are plotted in Figure 3. Slopes are negative, which is expected, as this indicates stronger ground motion for softer soils. Slopes also tend to increase with period over the range considered, which is also consistent with past experience (e.g., Boore et al. 1997 and Choi and Stewart 2005).

The results in Figure 3 indicate a break in the V_{S30} scaling for fast velocities and longer periods (e.g., as seen in the results for $T = 1.0$ s). It is this break in slope that motivated the use of the corner velocity V_c in the linear portion of the site amplification function (Equation 2). This important observation is driven by California and Japanese data; it has not been investigated by alternate means, such as simulations.

We plot in Figure 4 the slope parameter c for V_{S30}-scaling as a function of spectral period for the combined data set and several regions contributing substantial amounts of data. Since the regression for c is least-squares, all data points are weighted equally. Accordingly, the "combined" result is influenced strongly by regions with large amounts of data (principally California, Japan, and Taiwan). We find relatively consistent values of c for all regions, especially at short periods. For this reason, we do not include a regional adjustment for the c parameter in our model. As discussed further in the following section and Stewart and Seyhan (2013; hereafter, SS13), stronger regional variations in c can be found in Japan if different data-selection criteria are applied.

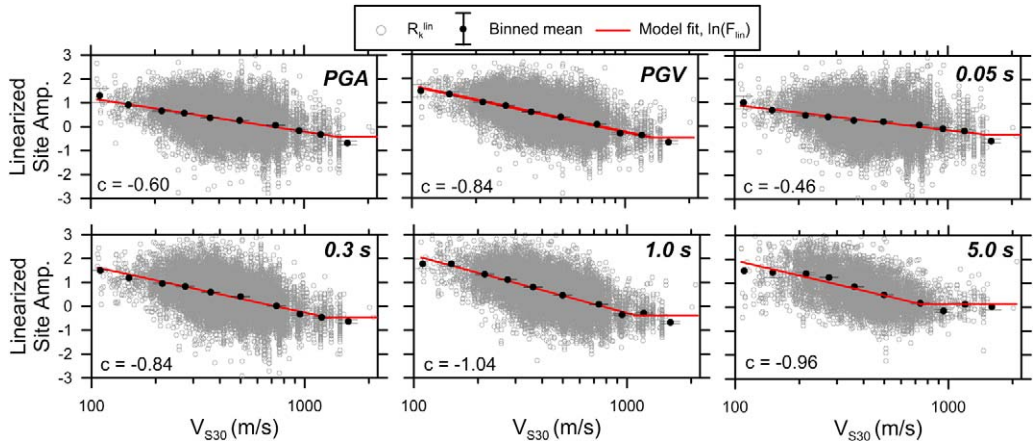

Figure 3. Variation of linearized site amplification (Equation 6) with V_{S30} for global NGA-West2 data set. Red line indicates model prediction. Binned means shown with their 95% confidence intervals.

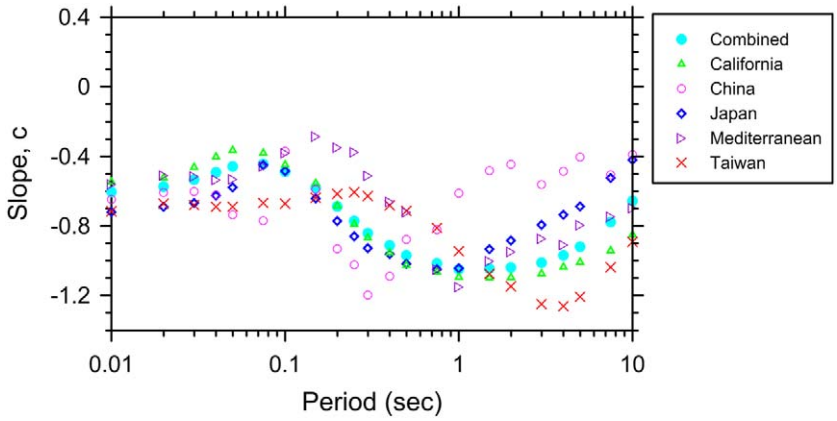

Figure 4. Variation of slope (c) within spectral periods for combined data set and various regions. Data weights refer to the relative contributions to the "combined" slope.

REGIONAL EFFECTS

Because the empirical data analyses performed to support the development of the site amplification model utilized a global data set, it is of interest to evaluate possible regional dependencies. Such analyses are complicated by known regional variations of anelastic attenuation (e.g., BEA14), which can introduce systematic bias in GMPE predictions at large distances for specific events. If not accounted for, this bias could be mistakenly mapped into site amplification using the data analysis procedures described previously. Such effects are particularly important for the analysis of the linear component of site amplification, which tends to be weighted toward the large number of sites at large distance where amplitudes of shaking are low.

This problem has previously been addressed by truncating the data set used for analysis of site response at site-source distances sufficiently small (approximately 80 km) that anelastic attenuation effects are unlikely to be significant (e.g., Campbell and Bozorgnia, 2014, Stewart et al. 2013). Our approach is different, opting instead to correct for regional anelastic attenuation effects and extend the distance range much further (up to approximately 400 km). The regional correction for anelastic attenuation is incorporated into the BEA14 GMPE used for residuals analysis in Equation 5 (i.e., it affects the reference rock mean μ_r).

Figure 5 shows the dependence of linearized site amplification (represented by R_k^{lin}) with V_{S30} for California and Japan, which contribute substantially to the NGA-West2 data set (additional regions were considered by SS13). The two data-selection criteria described previously were applied. Residuals R_k^{lin} were sorted by region and regressed using Equation 2 to obtain slope parameter c. These regressions were performed with V_{ref} left as a free parameter in order to obtain the most accurate slope. This causes the regression to be non-zero at 760 m/s, which is the desired reference velocity. That offset from zero at 760 m/s is subtracted on a regional basis for the plots in Figure 5.

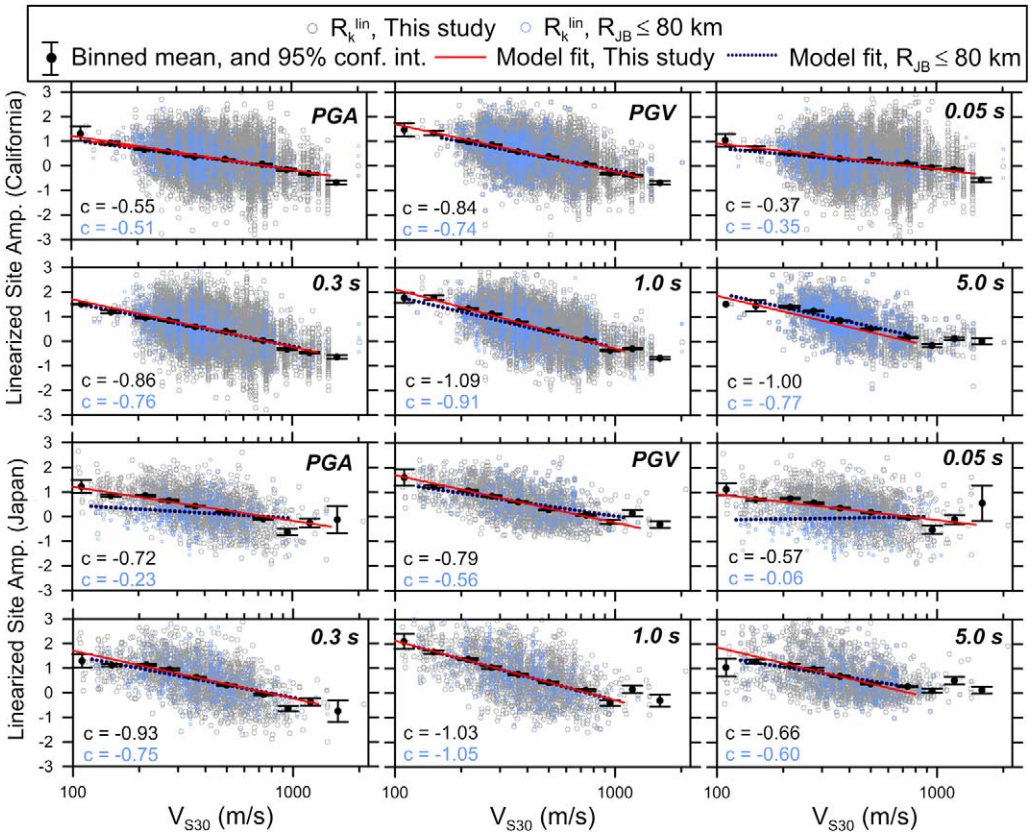

Figure 5. Variation of linearized site amplification (Equation 6 with V_{S30} for subsets of data from California and Japan. Trend lines shown for $V_{S30} < V_c$ are computed from data identified from the selection criteria in the present study (including large distances) and the $R_{JB} < 80$ km (more restrictive) criteria.

As shown in Figure 5, the two data-selection criteria produce similar slopes from California data; similar analysis by SS13 for additional regions (other than Japan) also generally show lack of sensitivity to data-selection criteria. Japan is a notable exception, with the 80-km truncated data set producing slopes that are much flatter at short periods. Similar sensitivites of the V_{S30} slope parameter to data-selection criteria have been observed previously by Chiou and Youngs (2012) for the Japanese data. Until the cause of these differences in slopes are better understood, we consider it prudent to use slopes derived from the larger data set employed in the present analyses.

As mentioned in the previous section, we consider the regional variations in the c parameter (evaluated using the proposed approach) to be insufficiently robust to justify the use of regional c terms for V_{S30}-scaling. However, we recognize that: (1) the variability of c terms is relatively high, especially at longer periods; and (2) our results for the c parameter in Japan

are difficult to reconcile with the findings of previous site-response studies pointing to unusually strong amplification of sites in Japan at short periods (e.g., Atkinson and Casey 2003, Ghofrani et al. 2013, Stewart et al. 2013, and Anderson et al. 2013). No doubt additional work on Japanese site response will be undertaken to better understand these issues.

Regional variations in the nonlinear component of site response were investigated by SS13. The analysis of nonlinearity places a premium on close-distance sites likely to be subject to nonlinear soil behavior. There are relatively few such sites, particularly when the data are subdivided regionally. While some inter-region variations were observed, they were not considered sufficiently robust to be included in the proposed site amplification model.

MODEL APPLICATION FOR BUILDING CODE SITE FACTORS

Most building codes use site amplification factors denoted F_a and F_v, which represent average site amplification within the period ranges of 0.1–0.5 s and 0.4–2.0 s, respectively. It should be recognized that application of these averaged site factors introduces a degree of approximation relative to period-specific site factors as contained in the NGA-West2 GMPEs. The F_a and F_v factors are typically applied to modify ground motions on hazard maps, which apply for a reference site condition of $V_{S30} = 760$ m/s (Frankel et al. 1996). As described by Seyhan and Stewart (2012), previous site factors in the NEHRP *Provisions* (BSSC, 2003) and used in building codes are biased with respect to site amplification from NGA-West1 GMPEs. There are two principal reasons for the discrepancies. First, previous NEHRP site factors were normalized relative to a reference velocity of 1,050 m/s, whereas they were applied relative the value of $V_{S30} = 760$ m/s used in national hazard maps. Second, the levels of nonlinearity and V_{S30} scaling are now different than what was evaluated in the early 1990s when the existing site factors were developed (Borcherdt 1994; hereafter, B94). We address these issues in the derivation of new site factors in this section.

The process of developing the new site factors was overseen by a working group formed as part of the NGA-West2 project and recognized by the BSSC *Provisions Update Committee* (PUC) as the body responsible for producing a proposal addressing this matter (working group members are listed in *Acknowledgments*). The site factors described here were approved by the PUC for publication in the 2015 NEHRP *Provisions*.

We apply the site amplification model described above to generate site amplification factors within the V_{S30} bins, and at the PGA_r values, currently used in the NEHRP *Provisions*. An additional set of factors for a stronger PGA_r level has also been included. The NEHRP site factors are specified for Categories A-E with the V_{S30} limits given in Table 2. We select representative V_{S30} values for each category as the median of measured values from the NGA-West2 site database (Seyhan et al. 2014), which are also shown in Table 2. Also shown for reference purposes are the values used by B94 and the geometric mean of category endpoints.

The rationale behind the selection of median V_{S30} values is that the NEHRP factors reflect the observed distributions of within-category site conditions. The resulting factors are not substantially different if they are evaluated at alternate velocities selected by B94 or at the geometric mean of the category limits.

Table 2. Velocity ranges in NEHRP categories and various representative V_{S30} values

NEHRP site class	NGA-West2 median V_{S30} (m/s)	Mid-range V_{S30} (m/s) from B94	Geometric mean of class limits (m/s)
E ($V_{S30} \leq 180$ m/s)	155	150	180
D (180 m/s < V_{S30} < 360 m/s)	266	290	255
C (360 m/s ≤ V_{S30} < 760 m/s)	489	540	523
B (760 m/s ≤ V_{S30} < 1,500 m/s)	913	1,050	1,068
A ($V_{S30} \geq 1{,}500$ m/s)	1,620[a]	1,620	1,500

[a]Adopted from Borcherdt (1994).

The NEHRP site factors are developed using the model represented by Equation 1. The $\ln(F_{lin})$ term is computed using Equation 2 by averaging slope (c) values across period ranges of 0.1–0.5 s (for F_a) and 0.4–2.0 s (for F_v). The averaging is not done across all NGA periods within those ranges, because they are not evenly sampled in log space. Rather, we selected 20 periods per log cycle that were (roughly) evenly sampled. The corresponding c values are -0.73 for F_a and -1.03 for F_v. Following extensive deliberation within the working group, we selected $V_{ref} = 760$ m/s, which is where the amplification is unity. A contrary opinion advocating the use of $V_{ref} = 1{,}050$ m/s is provided by Borcherdt (2014).

The $\ln(F_{nl})$ term is computed using Equation 3, in which slope f_2 is computed using Equation 4 from averaged f_4 and f_5 values for the respective period ranges computed as described above and for the V_{S30} values shown in Table 2.

Since reference site ground motion amplitudes are specified in the NEHRP *Provisions* in terms of spectral ordinates instead of PGA_r, we apply the following conversions:

$$S_s \approx 2.3 \times PGA_r$$
$$S_1 \approx 0.7 \times PGA_r, \tag{7}$$

The factors of 2.3 and 0.7 in Equation 7 are based on differences in the median spectral ordinates (e.g., 0.2 s PSA) relative to PGA from GMPEs for rock site conditions and typical ranges of **M** (6–8) and distance (<30 km) that control seismic hazard. These values are updated from 2.5 and 1.0 used with the previous NEHRP factors. The factor S_1/PGA is significantly **M**-dependent and the value of 0.7 corresponds approximately to **M**7.

Site factors computed using the above process are given in Figure 6. Also shown in Figure 6 are site terms from the NGA-West2 GMPEs and a site amplification model proposed for the pan-European region (Sandikkaya et al. 2013; SEA13) normalized to a common reference site condition of 760 m/s (using a procedure given in Seyhan and Stewart 2012). To be consistent with the site factor calculation, the GMPE and SEA13 site terms are computed at equally spaced periods on a log scale and averaged (in arithmetic units) for the plot in Figure 6.

For the case of Site Class A, we maintain the previous values of 0.8, which are generally consistent with amplification for $V_{S30} > V_c$. For Site Class E, median estimates of site

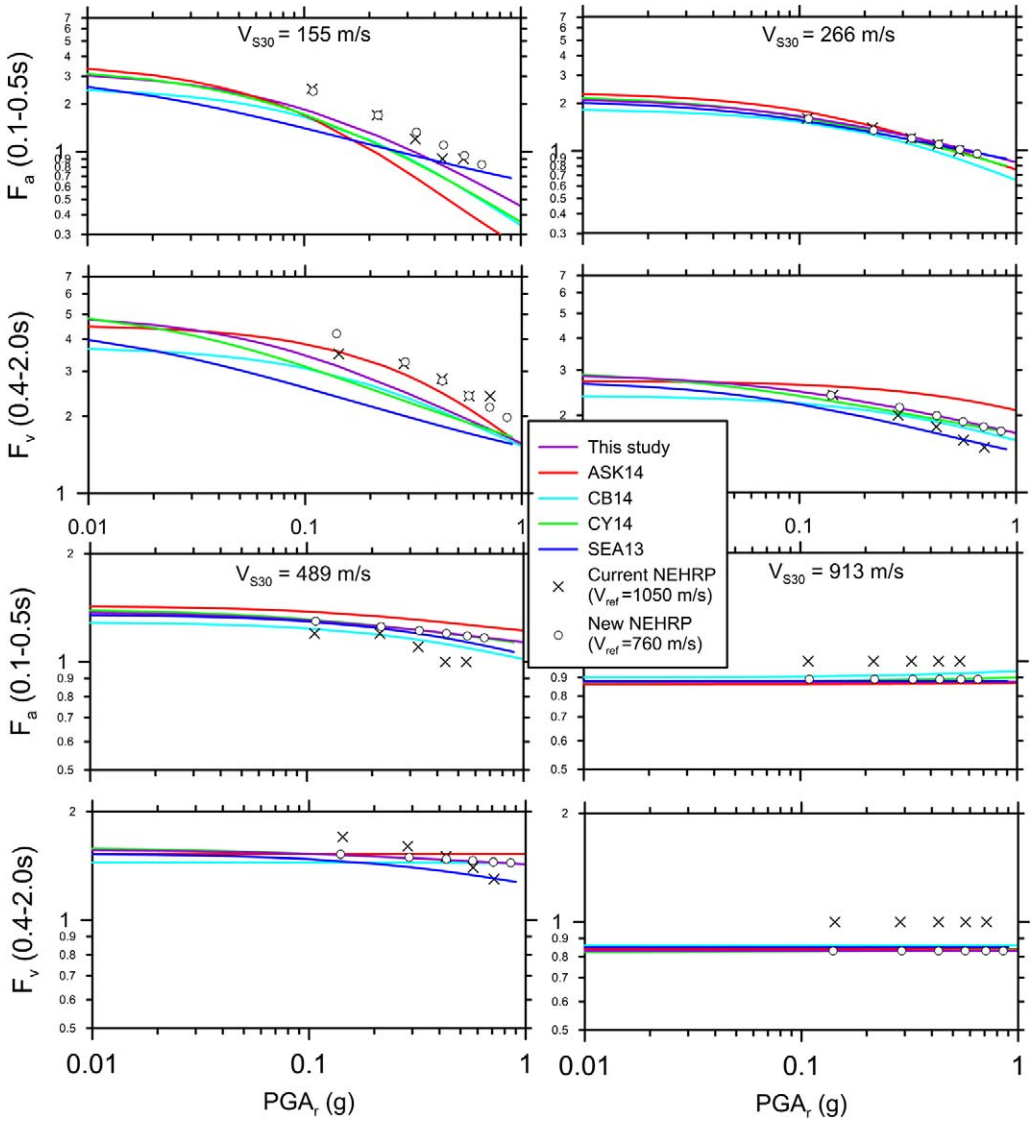

Figure 6. Comparison of proposed and current NEHRP site factors with site terms in NGA-West2 GMPEs and a European model (SEA13) normalized to a common reference site condition of $V_{ref} = 760$ m/s. ASK14 = Abrahamson et al. (2014); CB14 = Campbell and Bozorgnia (2014); CY14 = Chiou and Youngs (2014).

amplification were initially computed in the same manner as the other classes. However, the recommended factors for Site Class E are increased above the median by one-half of the within-event standard deviation derived from the data, which increases site factors by approximately a factor of 1.3–1.4. This introduces a conservative bias to the Class E factors that is considered desirable due to the relatively modest amount of data for this

site condition. A conservative bias was applied in the original site factors for Class E as well (Dobry et al. 2000). As shown in Figure 6, other than Class E, the recommended site factors are consistent with those in the NGA-West2 models. The SEA13 model is similar to our results except for Class E, where it has less nonlinearity and lacks saturation for low PGA_r in the range plotted.

For relatively weak levels of shaking, the proposed site factors are generally smaller than original values due to the change in reference velocity from 1,050 m/s to 760 m/s. For stronger shaking levels and Class C and D soils, the recommended site factors become close to, or slightly greater than, original values because of reduced levels of nonlinearity, especially at long period (i.e., in the F_v parameter).

The nonlinear model has a substantial effect on the computed factors for Class E. There are large epistemic uncertainties in this model, especially at long periods where the empirical and simulation results underlying the model are divergent. Our introduction of conservatism in the Site Class E factors, as described above, is intended to approximately account for this epistemic uncertainty.

Tabulated versions of the proposed site factors are given in the Electronic Supplement. The final published values deviate slightly from those plotted in Figure 6 due to round off to the nearest 0.1, which is customary in the NEHRP tables.

SUMMARY

We have developed semi-empirical site amplification equations applicable to regions having shallow crustal earthquakes. Site amplification is expressed as the sum (in natural log units) of terms representing the linear and nonlinear components of site response. The linear term represents V_{S30}-scaling and is evaluated empirically from the NGA-West2 data. The nonlinear component of the model is constrained jointly by NGA-West2 data and simulation results. We find the V_{S30}-scaling to show some regional variations, but the significance of those variations are strongly sensitive to the method of data selection. When regional anelastic attenuation effects are considered in the data analysis and the data is extended to large distances, regional site response effects are relatively modest (this is the adopted approach). On the other hand, when a relatively short cutoff distance is used to minimize anelastic attenuation effects (less than approximately 80 km), regional effects are much stronger, especially for Japanese data at short periods. The nonlinearity in site amplification does not show strong evidence of regional variability.

The complete model (for V_{S30}-scaling and nonlinearity) is used to derive NEHRP site factors using a reference velocity of 760 m/s. For relatively weak levels of shaking, the new NEHRP site factors are generally smaller than previous values due to the change in reference velocity from 1,050 to 760 m/s. For stronger shaking levels and Class C and D soils, the new site factors become close to, or slightly greater than, those used previously because of reduced levels of nonlinearity, especially at long period (i.e., in the F_v parameter). Factors for soft soil (Class E) were set conservatively, as were the original NEHRP site factors, to account for relatively large epistemic uncertainty in the nonlinearity for this site class. The site factors developed here have been approved by the Provisions Update Committee of the Building Seismic Safety Council and will appear in the 2015 version of the NEHRP *Provisions*.

ACKNOWLEDGMENTS

This study was sponsored by the Pacific Earthquake Engineering Research Center (PEER) and funded by the California Earthquake Authority, California Department of Transportation, and the Pacific Gas & Electric Company. Any opinions, findings, and conclusions or recommendations expressed in this material are those of the authors and do not necessarily reflect those of the above mentioned agencies. The work described in this report benefitted from discussions among the NGA-West2 Task 8 working group, consisting of Donald Anderson, Roger D. Borcherdt, Yousef Bozorgnia, Kenneth W. Campbell, C.B. Crouse, Robert W. Graves, I.M. Idriss, Maurice S. Power, Thomas Shantz, and Walter J. Silva. We thank all of the committee members for their dedicated efforts.

APPENDIX

Please refer to the online version of this manuscript to access the Electronic Supplements, which include: (1) a more detailed description of steps in model development related to interpreting simulations and constraining the f_3 parameter; (2) a table of the new NEHRP site factors developed in this manuscript; and (3) a table of model coefficients and a Matlab script that implements the site amplification model

REFERENCES

Afacan, K. B., Brandenberg, S. J., and Stewart, J. P., 2014. Centrifuge modeling studies of site response in soft clay over wide strain range, *J. Geotech. & Geoenvir. Eng., ASCE* **140**, 04013003.

Abrahamson, N. A., Silva, W. J., and Kamai, R., 2014. Summary of the ASK14 ground motion relation for active crustal regions, *Earthquake Spectra* **30**, 1025–1055.

Ancheta, T. D., Darragh, R. B., Stewart, J. P., Seyhan, E., Silva, W. J., Chiou, B. S.-J., Wooddell, K. E., Graves, R. W., Kottke, A. R., Boore, D. M., Kishida, T., and Donahue, J. L., 2014. NGA-West2 database, *Earthquake Spectra* **30**, 989–1005.

Anderson, J., Kawase, H., Biasi, G., and Brune, J., 2013. Ground motions in the Fukushima Hamadori, Japan, normal faulting earthquake, *Bull. Seismol. Soc. Am.* **103**, 1935–1951.

Atkinson, G. M., and Casey, R., 2003. A comparison of ground motions from the 2001 M 6.8 in-slab earthquakes in Cascadia and Japan, *Bull. Seismol. Soc. Am.* **93**, 1823–1831.

Boore, D. M., Joyner, W. B., and Fumal, T. E., 1997. Equations for estimating horizontal response spectra and peak acceleration from western North American earthquakes: A summary of recent work (with 2005 Erratum), *Seismol. Research Letters* **68**, 128–153.

Boore, D. M., and Atkinson, G. M., 2008. Ground motion prediction equations for the average horizontal component of PGA, PGV, and 5%-damped PSA at spectral periods between 0.01 and 10.0 s, *Earthquake Spectra* **24**, 99–138.

Boore, D. M., Stewart, J. P., Seyhan, E., and Atkinson, G. A., 2014. NGA-West2 equations for predicting PGA, PGV, and 5% damped PSA for shallow crustal earthquakes, *Earthquake Spectra* **30**, 1057–1085.

Borcherdt, R. D., 1994. Estimates of site-dependent response spectra for design (methodology and justification), *Earthquake Spectra* **10**, 617–653.

Borcherdt, R. D., 2014. Implications of next generation attenuation ground motion prediction equations for site coefficients used in earthquake resistant design, *Earthq. Eng. Str. Dyn.*, **43**, 1343–1360.

Building Seismic Safety Council (BSSC), 2003. *NEHRP Recommended Provisions for Seismic Regulations for New Buildings and Other Structures*, Part 1 (Provisions) and Part 2 (Commentary), Report prepared for the Federal Emergency Management Agency, Washington, D.C.

Campbell, K. W., and Bozorgnia, Y., 2014. NGA-West2 ground motion model for the average horizontal components of PGA, PGV, and 5% damped linear acceleration response spectra, *Earthquake Spectra* **30**, 1087–1115.

Chiou, B. S.-J., and Youngs, R. R., 2008. Chiou and Youngs PEER-NGA empirical ground motion model for the average horizontal component of peak acceleration and pseudo-spectral acceleration for spectral periods of 0.01 to 10 seconds, *Earthquake Spectra* **24**, 173–215.

Chiou, B. S.-J., and Youngs, R. R., 2012. Updating the Chiou and Youngs NGA model: Regionalization of anelastic attenuation, *Proc. 15th World Conf. Earthq. Eng.*, 24–28 September 2012, Lisbon, Portugal.

Chiou, B. S.-J., and Youngs, R. R., 2014. Update of the Chiou and Youngs NGA model for the average horizontal component of peak ground motion and response spectra, *Earthquake Spectra* **30**, 1117–1153.

Choi, Y., and Stewart, J. P., 2005. Nonlinear site amplification as function of 30 m shear wave velocity, *Earthquake Spectra* **21**, 1–30.

Dobry, R., Borcherdt, R. D., Crouse, C. B., Idriss, I. M., Joyner, W. B., Martin, G. R., Power, M. S., Rinne, E. E., and Seed, R. B., 2000. New site coefficients and site classification system used in recent building seismic code provisions (1994/1997 NEHRP and 1997 UBC), *Earthquake Spectra* **16**, 41–68.

Electrical Power Research Institute (EPRI), 1993. *Guidelines for Determining Design Basis Ground Motions*, Electrical Power Research Institute, Report No. EPRI TR-102293, Palo Alto, CA.

Frankel, A., Mueller, C., Barnhard, T., Perkins, D., Leyendecker, E. V., Dickman, N., Hanson, S., and Hopper, M., 1996. *National Seismic Hazard Maps: Documentation June 1996*, U.S. Geological Survey, USGS Open File Report 96-532, Denver, CO.

Ghofrani, H., Atkinson, G. M., and Goda, K., 2013. Implications of the 2011 M9.0 Tohoku Japan earthquake for the treatment of site effects in large earthquakes, *Bull. Earthq. Eng* **11**, 171–203.

Kamai, R., Abrahamson, N. A., and Silva, W. J., 2014. Nonlinear horizontal site amplification for constraining the NGA-West2 GMPEs, *Earthquake Spectra* **30**, 1223–1240.

Sandikkaya, M. A., Akkar, S., and Bard, P.-Y., 2013. A nonlinear site-amplification model for the next pan-European ground-motion prediction equations, *Bull. Seismol. Soc. Am* **103**, 19–32.

Seyhan, E., and Stewart, J. P., 2012. Site response in NEHRP Provisions and NGA models, in *Geotechnical Engineering State of the Art and Practice: Volume of Keynote Lectures from GeoCongress 2012*, Oakland, CA, ASCE Geotech. Sp. Pub. 226, K. Rollins and D. Zekkos (eds.), 359–379.

Seyhan, E., Stewart, J. P., Ancheta, T. D., Darragh, R. B., and Graves, R. W., 2014. NGA-West2 site database, *Earthquake Spectra* **30**, 1007–1024.

Stewart, J. P., and Seyhan, E., 2013. *Semi-Empirical Nonlinear Site Amplification and its Application in NEHRP Site Factors*, PEER Report No. 2013/13, Pacific Earthquake Engineering Research Center, University of California, Berkeley, CA, 59 pp.

Stewart, J.P., Midorikawa, S., Graves, R.W., Khodaverdi, K., Miura, H., Bozorgnia, Y., and Campbell, K. W., 2013. Implications of M_w 9.0 Tohoku-oki Japan earthquake for ground motion scaling with source, path, and site parameters, *Earthquake Spectra* **29**, S1–S21.

Walling, M., Silva, W. J., and Abrahamson, N. A., 2008. Non-linear site amplification factors for constraining the NGA models, *Earthquake Spectra* **24**, 243–255.

(Received 30 June 2013; accepted 13 February 2014)